

**Title: Astrocytes locally translate transcripts in their peripheral processes**

**Authors:** Kristina Sakers<sup>1-3</sup>, Allison M. Lake<sup>2,3</sup>, Rohan Khazanchi<sup>2,3</sup>, Rebecca Ouwenga<sup>1-3</sup>, Michael J. Vasek<sup>2,3</sup>, Adish Dani<sup>4,5</sup>, Joseph D. Dougherty<sup>2,3\*</sup>

**Affiliations:**

<sup>1</sup>Division of Biology and Biomedical Sciences, Washington University School of Medicine, USA.

<sup>2</sup>Department of Genetics, Washington University School of Medicine, USA.

<sup>3</sup>Department of Psychiatry, Washington University School of Medicine, USA.

<sup>4</sup>Department of Pathology, Washington University School of Medicine, USA.

<sup>5</sup>Department of Immunology, Washington University School of Medicine, USA.

**\*\*Correspondence to:** [jdougherty@genetics.wustl.edu](mailto:jdougherty@genetics.wustl.edu)

**One Sentence Summary:** Local translation in astrocytes.

# **Abstract:**

Local translation in neuronal processes is key to the alteration of synaptic strength that contributes to long term potentiation and potentially learning and memory. Here, we present evidence that astrocytes also have ribosomes in their peripheral and perisynaptic processes, that new protein synthesis is detectable in the astrocyte periphery, and that this localized translation is both sequence dependent and enriched for particular biological functions. Enriched transcripts include key glial regulators of synaptic refinement suggesting that local production of these proteins may support microscale alterations of adjacent synapses.

# **Main Text:**

Astrocytes are indispensable in the development and maintenance of the synapse- a structure described as tripartite due to the critical contribution from peripheral processes of these cells<sup>1</sup>. There is evidence that astrocytes determine synapse number<sup>2,3</sup>, and strength<sup>4,5</sup>, and complementary indications that neurons mediate maturation of astrocyte processes<sup>6</sup>. Yet, our understanding of these interactions is incomplete.

The localized synthesis of proteins in neurons is instrumental for synaptic modulation<sup>7</sup> and neurite outgrowth<sup>8,9</sup>. Because of the distances neurites must extend to reach a target cell, they have the ability to harbor mRNAs and ribosomes proximal to spines and axons<sup>10,11</sup> where local translation occurs in a precise spatial, temporal and activity-dependent manner. Additionally, oligodendrocytes also selectively localize some myelin associated mRNAs in their peripheral processes<sup>12</sup>.

Local translation in both neurons and oligodendrocyte processes suggests that other CNS cells may require this adaptation to compartmentalize functions within the cell. Peripheral astrocyte processes (PAPs) reach lengths comparable to that of some neurites and one astrocyte territory can contact up to 100,000 synapses<sup>13</sup>. Further, the dynamic action of PAPs at synapses requires rapid responsiveness to synaptic changes<sup>5,14</sup>. Therefore, we hypothesized that astrocytes also utilize local translation. We reasoned that four conditions must be met to support local translation in astrocytes: 1) ribosomes and 2) mRNA must be present in PAPs, 3) translation must occur in PAPs, and 4) be enriched for specific transcripts. Here, we provide biochemical and imaging evidence for these four criteria.

Previous work has suggested that ribosome-like structures exist in PAPs by electron microscopy(EM)<sup>15</sup>. We used transgenic mice where ribosomal protein Rpl10a is tagged with EGFP(Aldh1L1-EGFP/Rpl10a)<sup>16</sup> specifically within astrocytes to localize the large subunit of ribosomes *in vivo*. In cortical astrocytes, we found that EGFP/Rpl10a extends beyond Gfap+ processes and into peripheral processes surrounded by Aqp4, which marks astrocyte membranes and vascular endfeet<sup>17</sup>(Fig.1A,B). Further, we confirmed peripheral localization of endogenous small ribosomal subunits via immunofluorescence(IF) against Rps16(Fig.S1), indicating the tagged Rpl10a is not simply mislocalized in the Aldh1L1-EGFP/Rpl10a mice.

We next asked if we could detect tagged ribosomes in PAPs that were perisynaptic, using stochastic optical reconstruction microscopy(STORM)(Fig.1C). Astrocyte EGFP/Rpl10a was found within 100 nm of synapses, as defined by apposition of pre- and post-synaptic markers<sup>18</sup>.

Leveraging a viral method to sparsely GFP-label astrocytes in non-transgenic mice(Fig.1D), we also confirmed that mRNA localizes to PAPs. Previous colormetric *in situ* hybridization(ISH)

suggested that *Slc1a2* mRNA is localized peripherally,<sup>19</sup> and we confirmed this with fluorescent *in situ* hybridization(FISH)(Fig.1E).

After demonstrating the presence of both ribosomes and mRNA in PAPs, we next tested whether distal translation occurs by using puromycin to label actively-translated peptides in acute brain slices(Fig.2A). Using IF, we were able to detect nascent translation within PAPs, which was blocked by pretreatment with anisomycin, indicating that labeling requires active translation(Fig.2B). Given the short duration of incubation, we concluded that puromylylated peptides in PAPs were made locally rather than transported. Quantification of puromylation in astrocytes, either area or intensity, indicates 60% of translation in an astrocyte occurs > 9 microns from the nucleus (Fig. 2C, S2).

In neurons, local translation appears to be transcript-specific, often generating proteins with synaptic roles. If translation in PAPs does indeed have a physiological role, then specific transcripts should be translated there. To capture ribosome-bound mRNA from PAPs, we applied translating ribosome affinity purification(TRAP) to a synaptoneurosome(SN) preparation from *Aldh1L1:eGFP/Rpl10a* mice(Fig. 3A). Immunoblot confirmed depletion of nuclear protein LaminB2 and enrichment, as expected, of *Psd95* in the SN fraction. Additionally, we show the fraction contains Ezrin, a constituent of PAPs<sup>20</sup>, and astrocytic *EGFP/Rpl10a*(Fig. 3B). We used this affinity tag to harvest astrocyte ribosomes from the fraction, and performed RNA-seq(Table S1) on this sample('PAP-TRAP') and three comparison samples to identify PAP-enriched transcripts. Our analysis identified 224 transcripts that are significantly enriched on PAP ribosomes(Fig. 3C, Table S2), including *Slc1a2*, and 116 that are depleted('Soma' transcripts, Fig.3C, Table S3). These data establish that PAP fractions contain a distinct profile of ribosome-bound mRNAs(Fig. 3D). We confirmed the peripheral localization of several of these transcripts with FISH(Fig. 3E).

We then did a pathway analysis to identify possible functional consequences of local translation(Figs. 3F, S3). We found that PAP-localized transcripts had overrepresentation of genes mediating Glutamate and GABA metabolism, consistent with PAP functions of Glutamate transport(*Slc1a2*, *Slc1a3*)<sup>19,21</sup> and metabolism(*GluT*). Interestingly, we also noticed an enrichment for genes and members of gene families known to regulate synapse number(*Mertk*, *Sparc*, *Thbs4*)<sup>22-24</sup> suggesting that synapse formation and elimination may be mediated in part by local translation. Soma transcripts, by contrast, are enriched for transcription regulators and amino acid catabolism(Fig. S4).

Finally, we asked whether PAP-enriched transcripts contain sequence-specific features that may mediate localized translation. We found no differences in individual nucleotide or GC content(Fig. S5). However, PAP-enriched transcripts were significantly higher expressed in astrocytes compared to 'Soma' transcripts(Fig. 3G). In neurons, locally translated mRNAs, often sequestered by RNA-binding proteins(RBPs) into granules for transport and protection, have significantly longer 3'UTRs<sup>25</sup>. This may enable more sequence motifs or secondary structure for binding RBPs. We found that PAP-enriched transcripts are also significantly longer, specifically in their 3'UTRs(Fig. 3H), and that PAP-enriched 3'UTRs are predicted to have more stable secondary structures(Fig. 3I).

In summary, here we have clearly shown that substantial translation occurs peripherally in astrocytes and provided evidence that local translation is both enriched for particular functional categories and may be modulated by mechanisms involving specific features of the sequence. We

107 have also identified hundreds of candidates for local translation in astrocytes that warrant further  
108 targeted investigation, and future refinements to the PAP-TRAP method may further improve  
109 sensitivity to detect additional candidates and address alluring leads within the data(Fig.S9).  
110 Overall, these data lend support to the idea that an astrocyte contacting multiple synapses could  
111 use local translation to respond to or modulate the activity of specific synapses.

# Figures

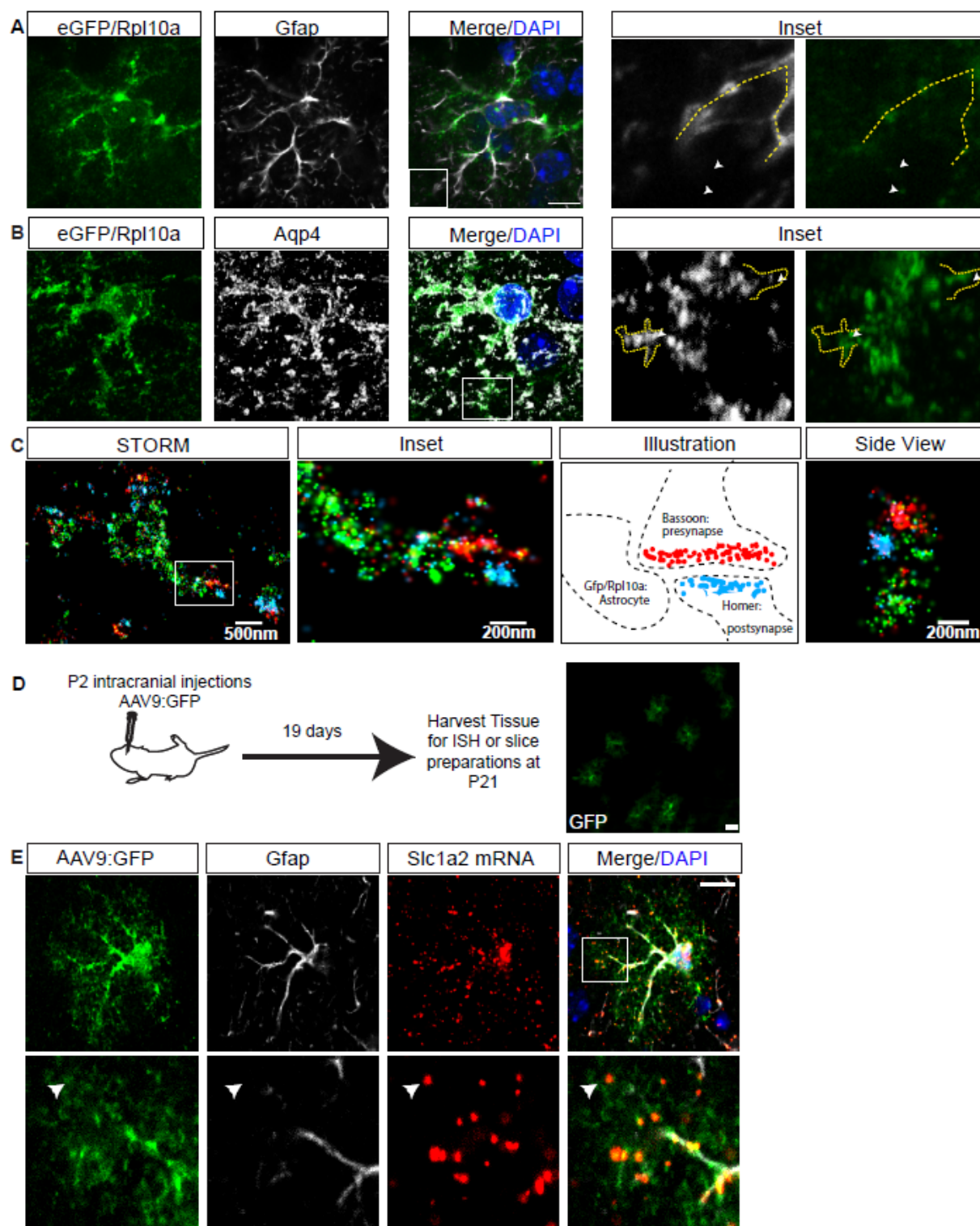


**Figure 1: Subcellular localization in cortical astrocytes shows ribosomal proteins and mRNA in peripheral processes** (A-B) Confocal IF of a cortical astrocyte, stained with Gfap(A) or Aqp4(B)(white). EGFP/Rpl10a(green) shows ribosomal tag extending throughout astrocyte, past Gfap+ processes (yellow dashed line) and within fine processes highlighted by Aqp4. Scale bar=10µm. (C) STORM imaging showing an EGFP/Rpl10a (green) filled astrocyte process proximal to synapses(as illustrated, these are defined by apposition of Bassoon(red), and Homer(blue)). Inset of box on left, and side view is a 90rotation of same, showing EGFP/Rpl10a puncta surrounding a synapse. (D) Early postnatal pups are injected transcranially with AAV9 expressing GFP, resulting in sparse labeling of cortical astrocytes after 3 weeks. Scale bar=20µm. (E) Confocal IF of a GFP-labeled astrocyte shows extension of *Slc1a2*(red) FISH into fine, Gfap(white) negative peripheral processes, scale bar=10µm.



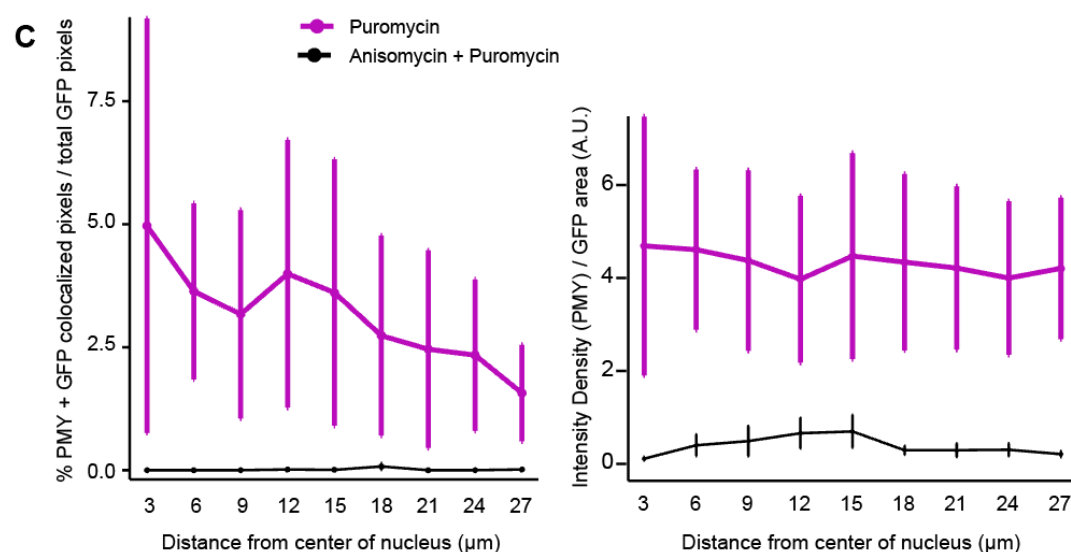
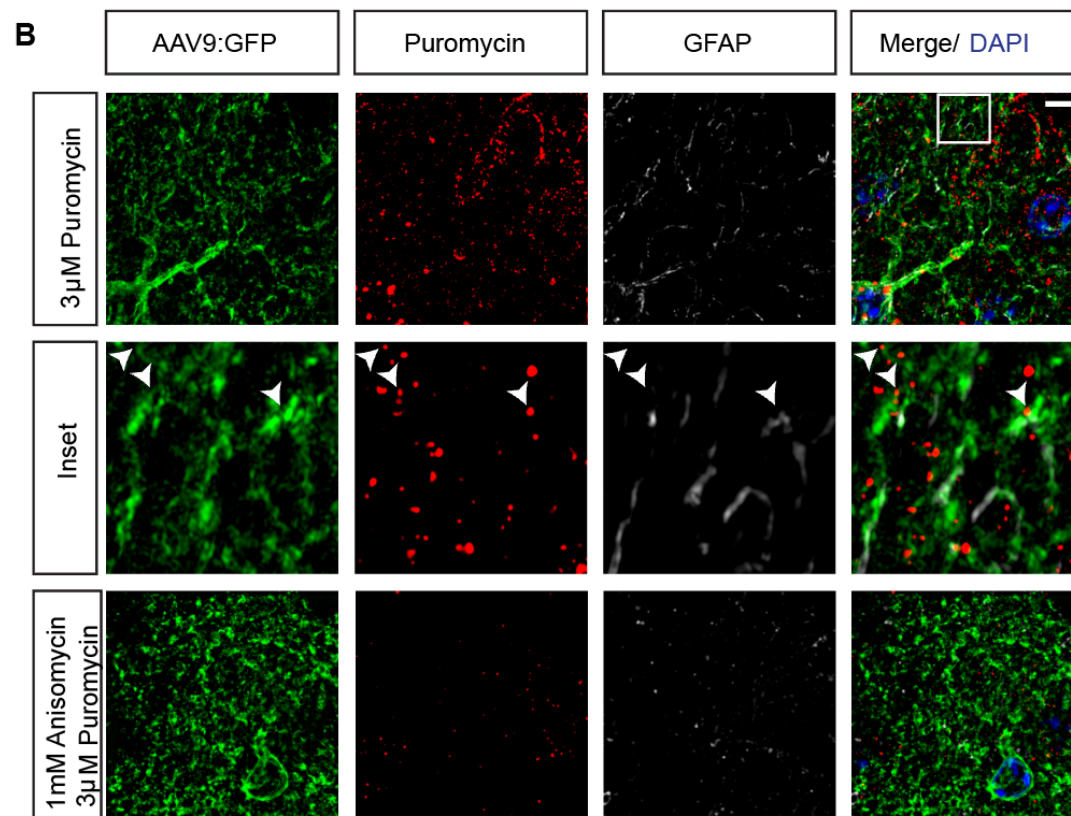
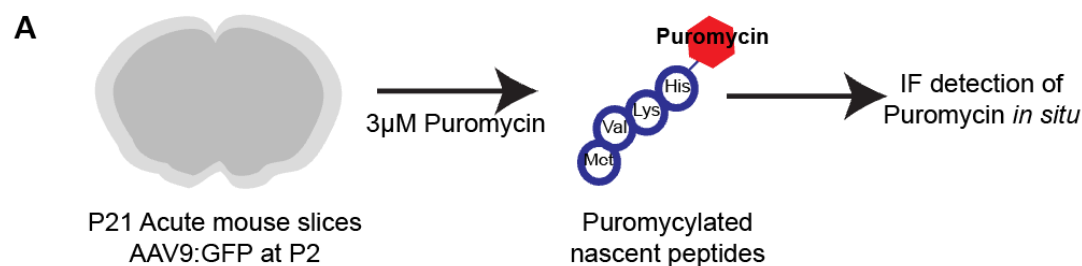


**Figure 2: Peripheral ribosomes are actively translating** (A) Acute slices(300  $\mu$ M) from P21 mice with sparse astrocyte labeling(generated as in Fig.1C), are treated for 10 minutes of puromycin, with or without 30 minutes of anisomycin pretreatment, then fixed, sectioned, and processed for IF against puromycin(red) and GFP(green). (B) Max projection super-resolution Structured Illumination Microscopy(SIM) to detect puromylation(violet) of synthesizing proteins in a GFP-labeled astrocyte shows translation occurs in peripheral processes, and is blocked by pretreatment with anisomycin. Scale bar=10 $\mu$ m. (C) Quantification of percent of GFP pixels colocalized with puromylation (PMY) pixels (left) and of intensity density of GFP and puromycin colocalized pixels (right), at increasing distance from nucleus indicates robust translation occurs in the periphery of astrocytes(Mean +/-SEM. N=11 and 10 cells for puromycin only and anisomycin pretreatment, respectively). No puromycin control had no puromycylated pixels(data not shown).



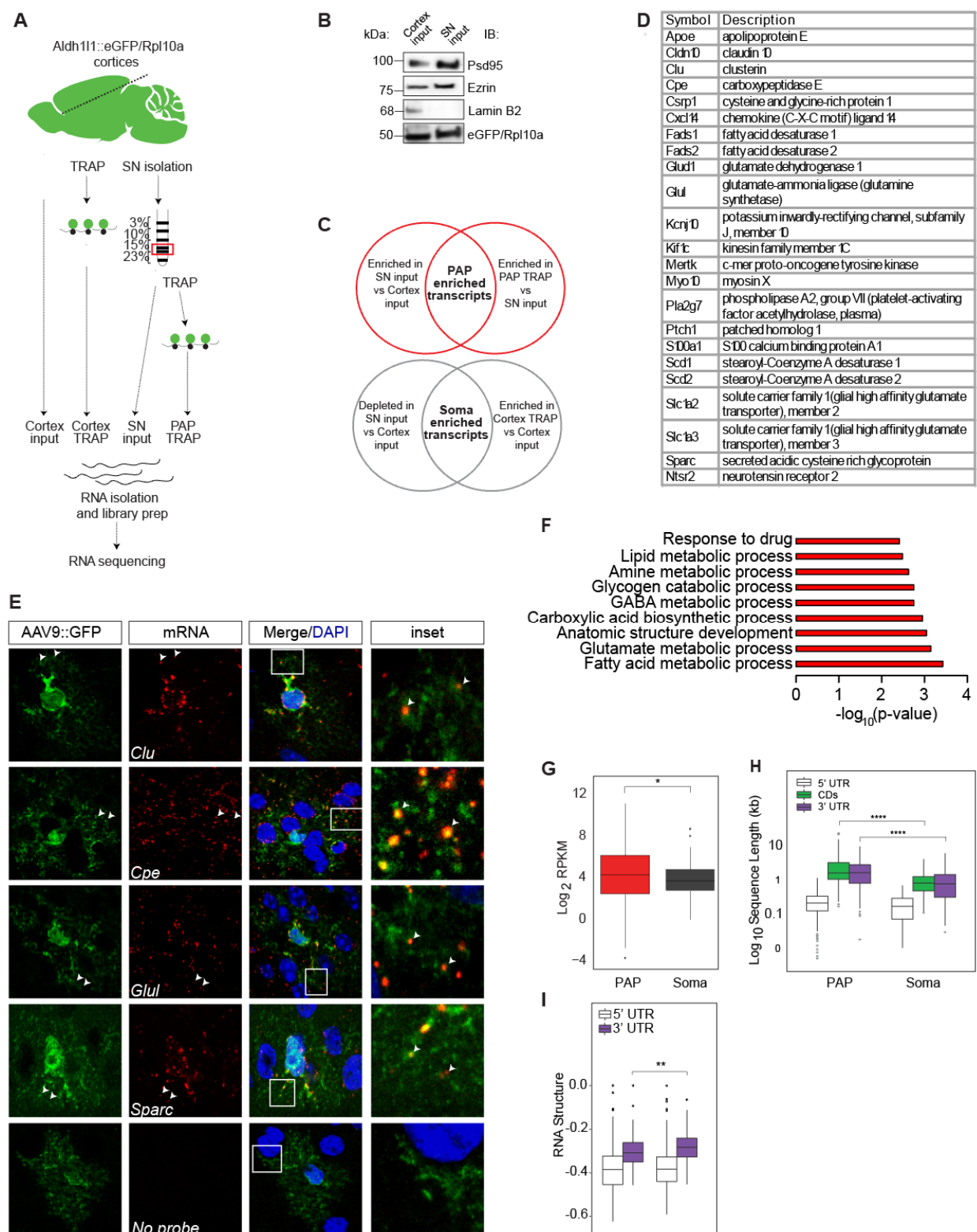


**Figure 3: Identification, pathway, and sequence analysis of peripherally enriched transcripts** (A) Diagram of experimental steps in PAP-TRAP and comparison samples for RNA-seq (B) Representative immunoblots for input and SN fraction confirms enrichment of synaptic

and PAP proteins, depletion of nuclear proteins (LaminB2) and presence of EGFP/Rpl10a (C) Diagram of analytical strategy for defining PAP and Soma enriched transcripts (D) Examples of PAP-enriched transcripts, including those related to Glutamate metabolism(*Slc1a2*, *Slc1a3*, *Glul*), fatty acid synthesis(*Fads*, *Scd*), and interesting signaling molecules(*Ptch1*, *Sparc*, *Ntsr2*). (E) FISH on GFP-labeled astrocytes confirms presence of PAP-TRAP identified mRNAs(*Cpe*, *Clu*, *Glul* and *Sparc*) in peripheral processes (F) Representative significant GO terms for PAP-enriched transcripts, hypergeometric test with Benjamini-Hochberg correction(B-H) (G) Quantification of expression of PAP-enriched and Soma-enriched transcripts indicates Soma transcripts have lower median expression in cortical astrocytes(Wilcoxon test, B-H corrected, \* $p < 0.05$ ) (H) Quantification of length of PAP and Soma transcripts indicates PAP-enriched transcripts have longer 3'UTRs(Wilcoxon test, B-H corrected, \*\*\*\* $p < 0.0001$ ). (I) RNA structure-score(minimum free energy of most stable predicted structure, normalized to length), indicates PAP-enriched transcripts have more stable 3'UTR secondary structures(Wilcoxon test, B-H corrected, \*\* $p < 0.01$ , lower values are more stable)

# **Acknowledgments:**

We thank Dr. Joshua Dearborn for help with the neonatal injections, Dr. Min-Yu Sun for guidance in preparing acute slices, Dr. Dennis Oakley and James Fitzpatrick for training and assistance with imaging, Dr. Kelly Monk for comments on the manuscript, and the members of the Dougherty lab for advice. This work was supported by the CDI(MD-II-2013-269, and a WUCCI Microgrant), NIH(DA038458-01, MH099798-01), WUSTL Interface of Psychology Neuroscience and Genetics Training Grant (5T32 GM081739) and WUSTL Neurosciences Program Training Grant (T32 GM008151). Key technical resources were provided by the Hope Center and the Genome Technology Resource Center at Washington University(supported by NIH grants P30 CA91842 and UL1TR000448), and the Washington University Center for Cellular Imaging(supported by CDI, St. Louis Children's Hospital, the Foundation for Barnes-Jewish Hospital, and NIH:NS086741).

# **Author contributions statement:**

RO developed and KS and RO refined the PAP-TRAP method. KS, AL, and JD designed and conducted bioinformatic analysis. RK, KS and JD conducted ISH, IF, imaging, quantification, and analysis. KS conducted and analyzed puromycylation studies. AD conducted STORM. MV developed image analysis pipeline for quantification. JD and KS conceived of study, designed experiments, and wrote manuscript.

# **Supplementary Materials:**

Materials and Methods

Figures S1-S7

Tables S1-S4 (.csv files)

# **References**

1. Araque, A. *et al.* Tripartite synapses: glia, the unacknowledged partner. *Trends Neurosci.* **22**, 208–215 (1999).

2. Ullian, E. M., Sapperstein, S. K., Christopherson, K. S. & Barres, B. A. Control of synapse number by glia. *Science* **291**, 657–661 (2001).
3. Mauch, D. H. *et al.* CNS synaptogenesis promoted by glia-derived cholesterol. *Science* **294**, 1354–1357 (2001).
4. Pfrieger, F. W. & Barres, B. A. Synaptic Efficacy Enhanced by Glial Cells in Vitro. *Science* **277**, 1684–1687 (1997).
5. Jourdain, P. *et al.* Glutamate exocytosis from astrocytes controls synaptic strength. *Nat. Neurosci.* **10**, 331–339 (2007).
6. Swanson, R. A. *et al.* Neuronal regulation of glutamate transporter subtype expression in astrocytes. *J. Neurosci. Off. J. Soc. Neurosci.* **17**, 932–940 (1997).
7. Kang, H. & Schuman, E. M. A requirement for local protein synthesis in neurotrophin-induced hippocampal synaptic plasticity. *Science* **273**, 1402–1406 (1996).
8. Kislauskis, E. H., Li, Z., Singer, R. H. & Taneja, K. L. Isoform-specific 3'-untranslated sequences sort alpha-cardiac and beta-cytoplasmic actin messenger RNAs to different cytoplasmic compartments. *J. Cell Biol.* **123**, 165–172 (1993).
9. Zhang, H. L. *et al.* Neurotrophin-induced transport of a beta-actin mRNP complex increases beta-actin levels and stimulates growth cone motility. *Neuron* **31**, 261–275 (2001).
10. Steward, O. & Levy, W. B. Preferential localization of polyribosomes under the base of dendritic spines in granule cells of the dentate gyrus. *J. Neurosci. Off. J. Soc. Neurosci.* **2**, 284–291 (1982).
11. Burgin, K. E. *et al.* In situ hybridization histochemistry of Ca<sup>2+</sup>/calmodulin-dependent protein kinase in developing rat brain. *J. Neurosci.* **10**, 1788–1798 (1990).

12. Colman, D. R., Kreibich, G., Frey, A. B. & Sabatini, D. D. Synthesis and incorporation of myelin polypeptides into CNS myelin. *J. Cell Biol.* **95**, 598–608 (1982).
13. Oberheim, N. A., Wang, X., Goldman, S. & Nedergaard, M. Astrocytic complexity distinguishes the human brain. *Trends Neurosci.* **29**, 547–553 (2006).
14. Mennerick, S. & Zorumski, C. F. Glial contributions to excitatory neurotransmission in cultured hippocampal cells. *Nature* **368**, 59–62 (1994).
15. Špaček, J. Ribosome-associated membrane contacts between astrocytes in the anoxic brain. *Acta Neuropathol. (Berl.)* **57**, 270–274 (1982).
16. Doyle, J. P. *et al.* Application of a translational profiling approach for the comparative analysis of CNS cell types. *Cell* **135**, 749–762 (2008).
17. Nielsen, S. *et al.* Specialized Membrane Domains for Water Transport in Glial Cells: High-Resolution Immunogold Cytochemistry of Aquaporin-4 in Rat Brain. *J. Neurosci.* **17**, 171–180 (1997).
18. Dani, A., Huang, B., Bergan, J., Dulac, C. & Zhuang, X. Superresolution Imaging of Chemical Synapses in the Brain. *Neuron* **68**, 843–856 (2010).
19. Danbolt, N. C., Storm-Mathisen, J. & Kanner, B. I. An [Na<sup>+</sup> + K<sup>+</sup>]-coupled glutamate transporter purified from rat brain is located in glial cell processes. *Neuroscience* **51**, 295–310 (1992).
20. Derouiche, A. & Frotscher, M. Peripheral astrocyte processes: monitoring by selective immunostaining for the actin-binding ERM proteins. *Glia* **36**, 330–341 (2001).
21. Rothstein, J. D. *et al.* Knockout of Glutamate Transporters Reveals a Major Role for Astroglial Transport in Excitotoxicity and Clearance of Glutamate. *Neuron* **16**, 675–686 (1996).

22. Chung, W.-S. *et al.* Astrocytes mediate synapse elimination through MEGF10 and MERTK pathways. *Nature* **504**, 394–400 (2013).
23. Kucukdereli, H. *et al.* Control of excitatory CNS synaptogenesis by astrocyte-secreted proteins Hevin and SPARC. *Proc. Natl. Acad. Sci. U. S. A.* **108**, E440–449 (2011).
24. Christopherson, K. S. *et al.* Thrombospondins Are Astrocyte-Secreted Proteins that Promote CNS Synaptogenesis. *Cell* **120**, 421–433 (2005).
25. Han, T. W. *et al.* Cell-free formation of RNA granules: bound RNAs identify features and components of cellular assemblies. *Cell* **149**, 768–779 (2012).